Abdominal Imaging

Published online: 8 May 2015

Abdom Imaging (2015) 40:2723–2737
DOI: 10.1007/s00261-015-0435-7

Multimodality fusion imaging in abdominal and pelvic malignancies: current applications and future perspectives

Francesco Paparo,[1] Arnoldo Piccardo,[2] Lorenzo Bacigalupo,[1] Riccardo Piccazzo,[1] Ludovica Rollandi,[1] Athena Galletto Pregliasco,[1] Marco Filauro,[3] Andrea DeCensi,[4] Gian Andrea Rollandi[1]

[1]Unit of Radiology, E.O. Ospedali Galliera, Mura della Cappuccine 14, 16128 Genoa, Italy
[2]Nuclear Medicine Unit, E.O. Ospedali Galliera, Mura della Cappuccine 14, 16128 Genoa, Italy
[3]Department of General and Hepatobiliary Surgery, E.O. Ospedali Galliera, Mura della Cappuccine 14, 16128 Genoa, Italy
[4]Unit of Oncology, E.O. Ospedali Galliera, Mura della Cappuccine 14, 16128 Genoa, Italy

Abstract

Medicine is evolving toward personalized care and this development entails the integration, amalgamation, and synchronized analysis of data from multiple sources. Multimodality fusion imaging refers to the simultaneous visualization of spatially aligned and juxtaposed medical images obtained by two or more image modalities. PET/MRI scanners and MMFI platforms are able to improve the diagnostic workflow in oncologic patients and provide exquisite images that aid physicians in the molecular profiling and characterization of tissues. Advanced navigation platforms involving real-time ultrasound are promising tools for guiding personalized and tailored mini-invasive interventional procedures on technically challenging targets. The main objective of the present essay was to describe the current applications and future perspectives of multimodality fusion imaging for both diagnostic and interventional purposes in the field of abdominal and pelvic malignancies. We also outlined the technical differences between fusion imaging achieved by means of simultaneous bimodal acquisition (i.e., integrated PET/MRI scanners), retrospective co-registration, and multimodality fusion imaging involving ultrafast or real-time imaging modalities.

Key words: Fusion imaging—Navigation—Magnetic resonance imaging—Choline—Positron emission tomography

Correspondence to: Francesco Paparo; *email:* francesco.paparo.ge@gmail.com; francesco.paparo@galliera.it

In the traditional model of radiology practice, imaging studies were analyzed, interpreted, and reported using hardcopy images displayed on view boxes. Until recently, therefore, physicians used to combine morphological, functional, and metabolic information obtained from different imaging modalities, acquired at different times, using a process called mental co-registration [1]. This process consists of finding adequate spatial correspondence between the pathological findings demonstrated by the relevant images from different modalities. Currently, softcopy digitalized images displayed on monitors are the first step of analysis. The wide availability of dedicated workstations for multimodality reading, interpretation, and reporting (e.g., single- and dual-screen workstations) allows diagnostic images from different modalities to be visualized side-by-side on the same high-resolution monitor display, thus making the process of mental co-registration smarter and more immediate [1, 2]. Nevertheless, as it mainly relies on the reader's skills and experience, it remains inexact and prone to human inaccuracies, particularly when the reader has to assess multiple lesions. The term multimodality "fusion imaging" (MMFI, also called "image fusion") refers to the simultaneous visualization of spatially aligned and juxtaposed medical images obtained by two or more image modalities [3]. This technique depends on the precise spatial co-registration of different image sets and provides a single fused image that is more informative and valuable than individual, separate assessment [4]. The acquisition of image sets to be fused may be either simultaneous (i.e., integrated scanners) or sequential with variable time intervals between the different modalities.

In this latter case, the fusion of previously acquired imaging studies is defined as "retrospective" [3–6]. In addition, by means of dedicated fusion imaging platforms, it is possible to combine and integrate real-time ultrasound with previously acquired cross-sectional imaging, including computed tomography (CT), magnetic resonance imaging (MRI), and positron emission tomography (PET) [7]. In the field of oncology, MMFI has several clinical applications for both diagnostic and interventional purposes. Non-invasive morphological and functional information can be used not only for the detection and staging of tumors, but also for personalized, tailored, and targeted therapy and treatment monitoring. From a diagnostic point of view, MMFI is able to improve the molecular profiling of tissues, assisting in their comprehensive and accurate non-invasive characterization. From the interventional point of view, MMFI can be successfully employed to assist percutaneous procedures for the biopsy or ablation of technically challenging targets, especially those characterized by low conspicuity on unenhanced CT and B-mode ultrasound images [8, 9]. The main objective of the present essay was to describe the current applications and future perspectives of MMFI for both diagnostic and interventional purposes in the field of abdominal and pelvic malignancies. We also outlined the technical differences between fusion imaging achieved by means of simultaneous bimodal acquisition (i.e., integrated PET/MRI scanners), retrospective co-registration, and MMFI involving ultrafast or real-time imaging modalities (i.e., ultrasound and cone beam CT).

Technical overview

MMFI can be defined as the process of co-registering and overlaying multiple images from single or multiple modalities [10]. Therefore, MMFI encompasses a broad range of techniques. An immediate example of fusion is the direct overlaying of two different images from the same modality that have been acquired during the same examination. This is the case of the overlaying of a functional color-coded map [e.g., the map of apparent diffusion coefficient (ADC) values obtained from diffusion-weighted MRI sequences] on a morphological sequence, thus allowing precise anatomical localization of suspected areas (Fig. 1A, B). This is the smartest form of fusion, since the two image series belong to the same examination and have the same spatial reference system, which is encoded in the digital imaging and communications in medicine (DICOM) files. Co-registration is the preliminary technical step necessary to perform MMFI and combine functional and metabolic information obtained from different modalities at different times, and ensures that the pixels from the various image sets represent the same volume with acceptable precision [11, 12]. It consists of the computational process that allows a precise correspondence to be found between the reference system (i.e., spatial coordinates) of an image set and that of another image set. In the co-registration process, a "floating" image is moved and/or deformed in order to obtain adequate matching and juxtaposition with a "reference" image [13]. Registration can be rigid or elastic (deformable) [5, 14]. Only translation and rotation are possible with rigid co-registration, whereas rotation, translation, and localized stretching are available with elastic co-registration, which improves the matching of anatomical structures [4]. Elastic co-registration techniques are useful when MMFI involves anatomical regions that may show substantially different dynamic physiological conditions (e.g., degree of filling of the urinary bladder, distension of bowel loops) among different imaging studies [15] (Fig. 1C, D). The computational techniques dedicated to compensation for shift/deformation of internal organs and breathing-related movements of peridiaphragmatic structures represent ongoing challenges to improve co-registration and fusion [8, 9, 16]. Three main forms of MMFI can be identified on the basis of the technique of acquisition of the image sets that are used as primary inputs for co-registration: simultaneous acquisition, retrospective fusion, and MMFI involving ultrafast or real-time modalities (i.e., virtual navigation).

Simultaneous acquisition and retrospective fusion imaging

Until recently, PET and MRI were considered mutually exclusive imaging techniques, not eligible for simultaneous acquisition owing to incompatible hardware requirements. Recently, however, hybrid PET–MRI systems, either simultaneous or sequential, have been developed in order to bring these imaging principles together [17, 18]. New combined PET/MRI scanners provide the simultaneous acquisition of both imaging modalities by performing an automated co-registration process with perfect temporal correlation of dynamically acquired datasets and MRI-based attenuation correction [19]. A PET detector ring placed within a 3.0T magnet is the hardware core of fully integrated single-gantry systems. Significant technical improvements to these scanners include the design and implementation of MRI-compatible PET photodetectors, techniques for maintaining magnetic field homogeneity and novel MR-based attenuation correction of PET data [19, 20]. MRI may substantially improve the reconstruction, interpretation, and analysis of PET data and this new integrated technique is expected to provide some advantages over PET–CT, which is a well-established modality in the field of oncological imaging. Compared with CT, MRI provides a better functional analysis for soft tissue characterization, which mainly relies on diffusion-weighted imaging (DWI), spectroscopy, and dynamic perfusion studies

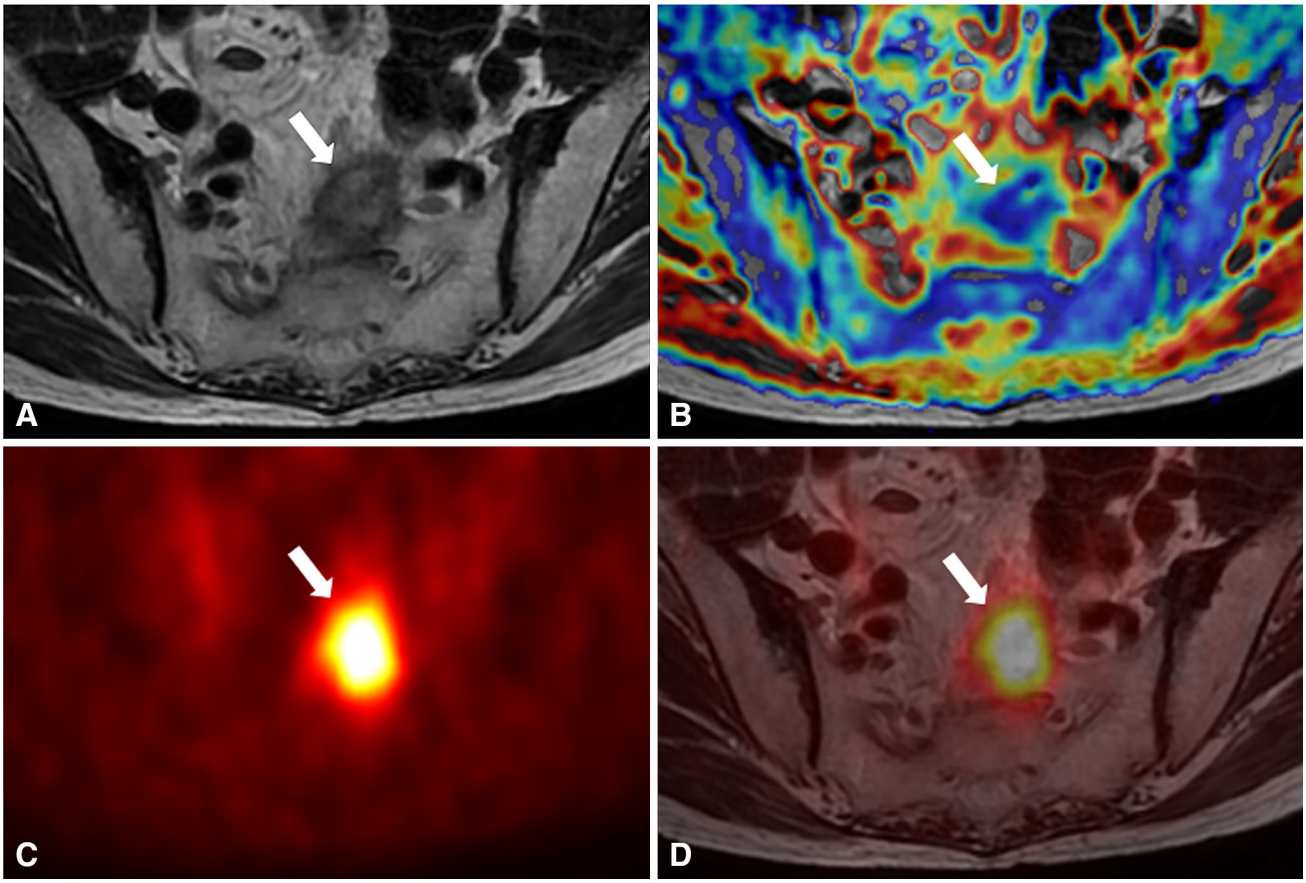

Fig. 1. 79-year-old woman who had undergone surgery 2 years earlier for an adenocarcinoma of the upper third of the rectum. The T2-weighted axial image **A** shows a presacral hypointense solid nodule suspect for local cancer recurrence. The ADC map juxtaposed and fused on the T2-weighted image **B** well demonstrates that the nodule is characterized by restricted water diffusion (*arrow*). The ^{18}F-FDG PET axial image **C** demonstrates a focal accumulation of the tracer (*arrow*) with a SUV_{max} of 16.8. The ^{18}F-FDG PET axial scan has been co-registered with elastic modality and fused with the T2-weighted axial image. The bimodal fused PET/MRI image **D** shows a precise spatial correspondence between the focal accumulation of the tracer ^{18}F-FDG and the presacral solid tissue (*arrow*). All images obtained with SmartFusion (Camelot Biomedical Systems, Genoa, Italy).

[21, 22]. Another major advantage of PET/MRI over PET/CT systems is the absence of radiation burden. Moreover, the simultaneous acquisition of PET and MRI data enable proper co-registration of dynamic and moving physiological conditions, and this is especially important in the assessment of the abdomen and pelvis, where the relative positions of organs may be altered owing to peristaltic motion and filling of the urinary bladder [4, 15]. Therefore, simultaneous PET/MRI acquisition is able to offer exquisite structural and functional/metabolic images. However, these expensive systems are not widely available, being mainly limited to research facilities [14–17]. Retrospective MMFI allows the co-registration of two or more image sets acquired at different times [9, 11]. It can be performed by means of a large variety of dedicated software platforms that employ either rigid or elastic co-registration techniques and can be installed on common radiological workstations (Fig. 2). Table 1 summarizes the advantages and limitations of simultaneous acquisition with PET/MRI scanners vs. retrospective fusion. Currently, the main potential future role of combined PET/MRI scanners seems to be the integration of local, nodal, and whole-body staging of tumors in a single "one-stop shop" modality, while avoiding the use of ionizing radiation [23]. On the other hand, dedicated software platforms for retrospective fusion are a low cost and valid alternative that allow us to bring MMFI out of research facilities and into routine clinical practice.

Virtual navigation

The last form of MMFI involves real-time or ultrafast imaging techniques (i.e., ultrasound and fluoroscopy) [24, 25]. It finds its main application in the field of minimally invasive percutaneous interventional procedures, including biopsy and tumor ablation. In recent years, MMFI guidance for interventional procedures has been

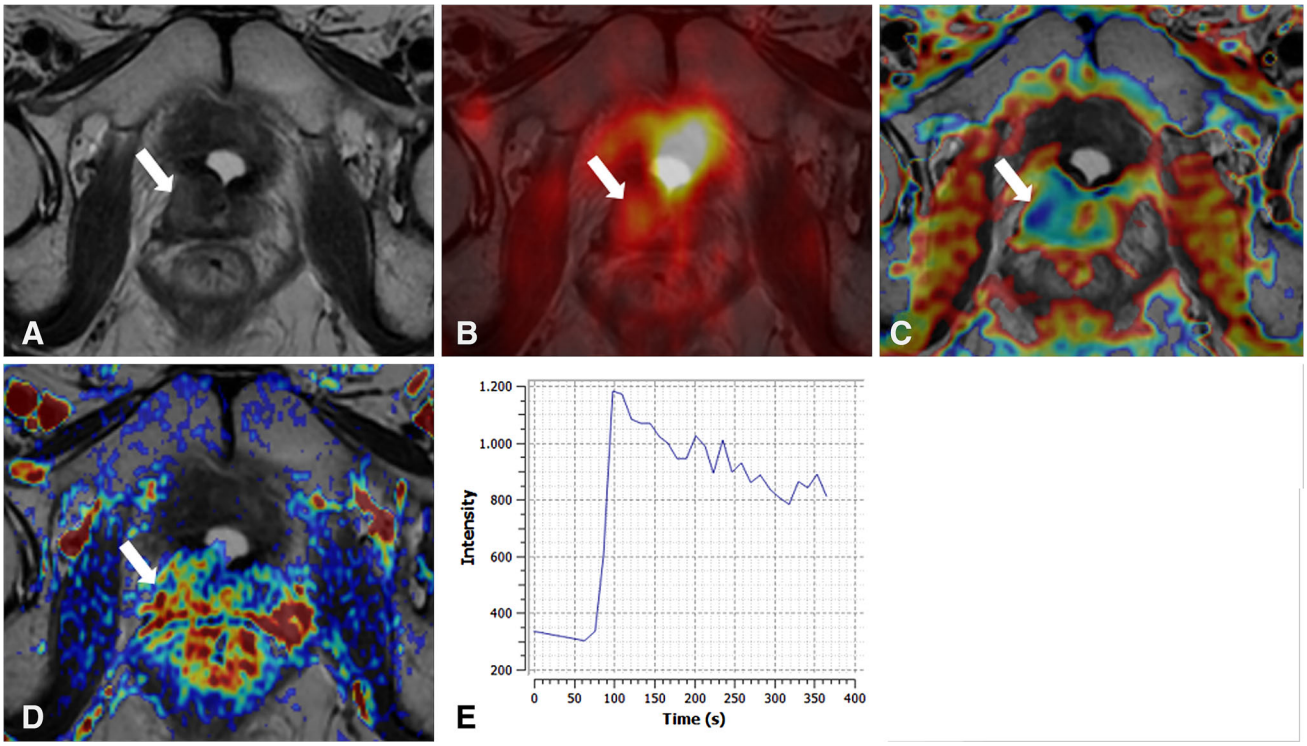

Fig. 2. 76-year-old man affected by biochemical recurrence 14 months after external beam radiation therapy for prostate cancer Gleason 8 (4 + 4). Signs of a previous TURP are also present. Current PSA value of 5 ng/mL with PSA doubling time <6 months. The T2-weighted axial image **A** demonstrates a hypointense nodular thickening of the right lobe of the prostate gland (*arrow*). The bimodal fused ^{18}F-choline PET/MRI axial image **B** demonstrates a clear accumulation of the tracer in the right lobe of the prostate (*arrow*). On the ADC map **C**, a nodular area of restricted water diffusion is well appreciable (*arrow*). On the perfusion map **D**, the suspect area is hypervascular (*arrow*) with a dynamic perfusion curve of type 3 (wash-out after initial upslope on the time/intensity graph), which is highly suggestive of cancer (**E**). Images obtained with the QuantaProstate (Camelot Biomedical Systems, Genoa, Italy).

assessed in several medical specialties and in various anatomical regions and organ systems [3]. Software modules for co-registration of real-time ultrasound images with pre-procedural contrast-enhanced CT, MRI, or PET/CT studies are implemented in several high-end multipurpose ultrasound machines [9]. By incorporating ultrasound into fusion imaging guided interventions, it is possible to combine the value of real-time, radiation-free intra-procedural monitoring with the peculiar advantages offered by panoramic cross-sectional imaging modalities, which are able to show the critical structures surrounding the target lesion [5, 7]. In addition, MMFI guidance enables target lesions with absent or low conspicuity on B-mode ultrasound images to be depicted, as happens in the case of some PET-positive lesions [8, 9].

Datasets that are used to generate fused images have first to be spatially aligned in order to achieve correct juxtaposition. The process of co-registration involving real-time ultrasound can be manual, semiautomatic, or automatic, with rigid or elastic methods being used to match a pre-procedural image set to intra-procedural or post-procedural B-mode ultrasound images [5, 7, 14]. Automatic methods analyze the intensity of voxels and pixels of the image sets to be fused, in order to find the orientation that minimizes the difference between them (e.g., by calculating the standard deviation of the ratio of voxel intensities) [11]. Automatic methods have been variably defined in the literature as voxel similarity measures, mutual information, or correlation ratios [3]. By contrast, manual methods require the operator to define, on both modalities, a series of reference registration points or matching landmarks, which may be either external (i.e., fiducial markers placed on the patient's skin) or internal (i.e., common anatomical structures, such as large vessels) [3, 9]. While manual methods may be more accurate, they are more time-consuming than automated ones (Fig. 3). Some manufacturers combine both methods by means of a first-pass rough automation followed by manual fine-tuning. Electromagnetic (EM) tracking enables us to monitor, in real-time, the position of the ultrasound probe in the virtual tridimensional workspace created by an EM field generator, thus creating the technical environment for the spatial alignment and co-display of B-mode ultrasound images with a second modality (i.e., virtual navigation) [7]. In EM tracking, a generator creates a magnetic field that represents a virtual work volume of

Table 1. Simultaneous and retrospective image fusion

Simultaneous acquisition (PET–MRI scanners)		Retrospective image fusion (dedicated software platforms)	
Advantages	Limitations	Advantages	Limitations
"One-stop shop" modality	Expensive	Elaboration and analysis of previously acquired image datasets	More time-consuming
Combination of whole-body MRI and PET	Not widely available	Not requiring the physical presence of MRI, CT and PET/CT scanners	Partial compensation for different physiological conditions (bowel peristalsis and different degrees of filling of the urinary bladder)
Less time-consuming		Less expensive	
Acquisition of the two modalities in the same physiological conditions		Widely available	
Automatic compensation for bowel peristalsis and different degrees of filling of the urinary bladder			
Whole-body MRI and PET			

Advantages and limitations of simultaneous acquisition with PET/MRI scanners vs. retrospective image fusion by means of dedicated software platforms

approximately 500 mm × 500 mm × 500 mm [14, 26]. A coil within this magnetic field produces a weak detectable electrical current, whose signal strength is related to the coil's position within the virtual workspace. The coil's location can be precisely mapped within a Cartesian coordinate system in a way similar to common GPS-based satellite navigation systems. Several coils can be tracked simultaneously [14, 26]. The coils are integrated in ultrasound probes, medical instruments, and fiducial skin patches. MMFI-guided interventions can be optimized and made less dependent upon the individual operator's experience using EM instrument tracking techniques in combination with real-time virtual navigation [5]. Therefore, EM tracking can be employed to determine the precise position of instruments and medical devices, such as biopsy needles and ablation catheters, during MMFI-guided interventional procedures and to display it in real-time over the multimodal fused images. Cone beam CT (CBCT)-based navigation technology relies on the co-registration between an intra-procedural three-dimensional CBCT dataset, generated in the angiography/fluoroscopy C-arm suite, and live fluoroscopy. Other cross-sectional imaging modalities, such as CT, MRI, and PET/CT, can be co-registered with intra-procedural CBCT, thereby allowing the operator to reference the multimodal fused images during live fluoroscopy and combine MMFI guidance with the advantages of ultrafast x-ray monitoring [27, 28]. CBCT navigation has been used to guide ablation procedures in oncological patients, but to date, this technique needs to be more extensively validated in the field of abdominal oncology.

Clinical value of diagnostic multimodality fusion imaging in abdominal and pelvic malignancies

Both PET and MRI are well-established imaging modalities that find many clinical applications in the field of oncology. The combination of PET with unenhanced CT for attenuation correction and anatomical localization has brought hybrid imaging into routine clinical practice [17]. The diagnostic advantages provided by integrating anatomical, functional, and metabolic information have led to the development of combined PET/MRI scanners and MMFI platforms. Nearly, a decade after the introduction of PET/CT, PET/MRI scanners for simultaneous acquisition have become commercially available [18]. These new scanners combine the high sensitivity of PET/CT in the detection of cancer with the unique features offered by MRI in the characterization of soft tissues; these include excellent contrast resolution, options for multiparametric and functional imaging techniques (e.g., dynamic contrast-enhanced perfusion studies and DWI), and the absence of ionizing radiation [21–23]. The clinical value of retrospective fusion imaging has already been assessed in various types of tumors and anatomical regions/organ systems, while the individual value of simultaneous PET/MRI in specific oncologic diseases in the abdomen and pelvis is still under investigation. Therefore, in this section, we will address both simultaneous PET/MRI and retrospective fusion imaging separately, but we will use the generic term PET/MRI fusion when addressing issues and concerns that may be considered common to both modalities. Simultaneous PET/MRI can be an effective imaging tool for accurate T-staging of those tumors in which MRI is routinely employed, in that it offers the benefit of comprehensive whole-body N- and M-staging in a single examination [21].

General advantages of multimodal fusion imaging in TNM staging

Peculiar advantages are expected in the post-surgical follow-up of patients; in this setting, PET/MRI may be

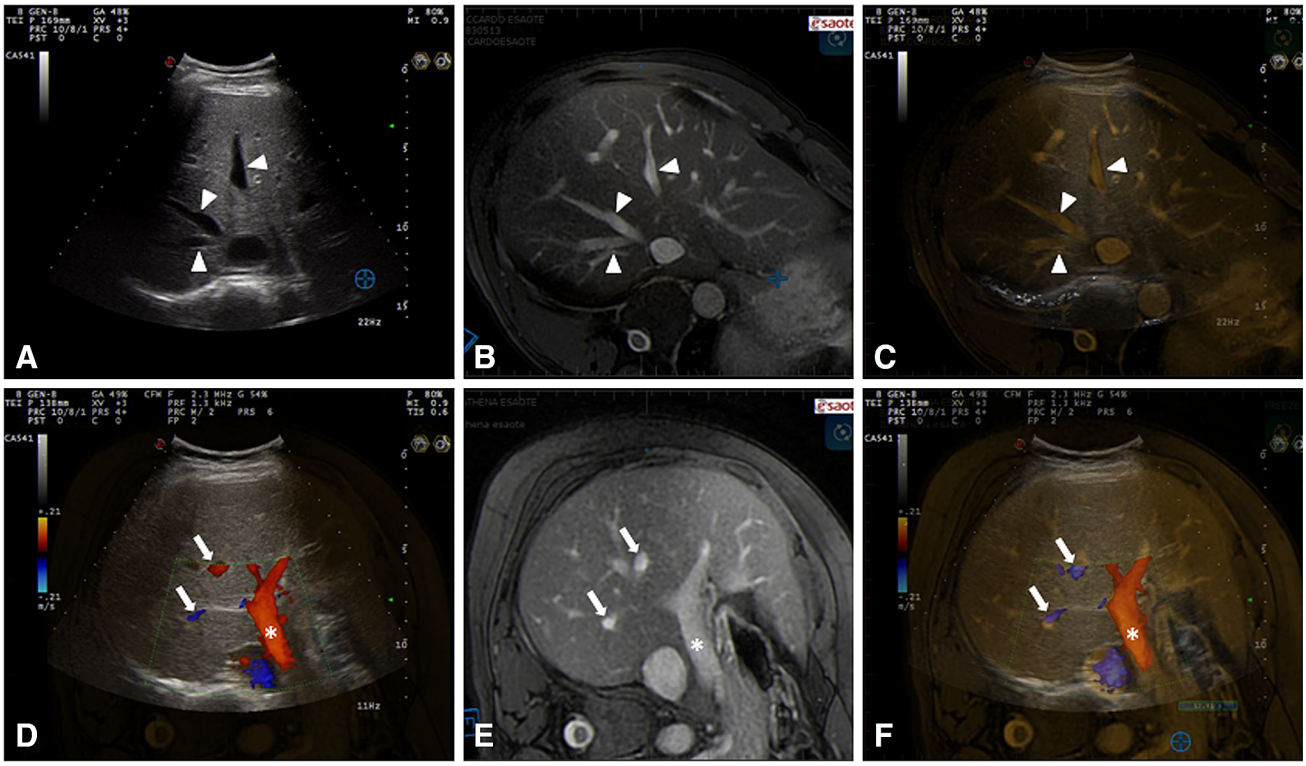

Fig. 3. 31-year-old healthy volunteer. Examples of real-time co-registration of B-mode ultrasound with a previously acquired fat-suppressed FIESTA MRI sequence by means of the Virtual Navigator platform implemented on the MyLab Twice ultrasound system (Esaote Biomedica, Genoa, Italy). The B-mode ultrasound scan **A** shows the three supra-hepatic veins (*arrowheads*). These vascular landmarks (*arrowheads*) are well appreciable also on the MR image **B** that is displayed by the software platform in the same dimension and cut-plane as the B-mode ultrasound image. The bimodal fused MRI/ultrasound image **C** demonstrates a precise juxtaposition of the internal vascular landmarks between the two modalities (*arrowheads*). The ultrasound image with the color-Doppler module **D** demonstrates the right branch of the portal vein (*asterisk*) and two small intrahepatic portal branches (*arrows*). These vascular landmarks are also displayed on the fat-suppressed FIESTA MR image (**E**). The bimodal fused MRI/ultrasound image (F) demonstrates precise juxtaposition of the internal vascular landmarks used as reference points for the real-time co-registration between the two imaging modalities.

used to distinguish a local recurrence of rectal cancer from fibrous scar tissue by combining the morphological and functional information of contrast-enhanced MRI and DWI with the metabolic information of ^{18}F-FDG PET [23] (Fig. 4). With regard to N-staging, ^{18}F-FDG PET/CT has improved the anatomical localization of PET abnormalities and reduced the number of equivocal PET interpretations, gradually becoming the reference modality for detecting metastatic lymph nodes in various types of cancer [29, 30]. However, ^{18}F-FDG activity is not specific to cancer, since macrophages involved in inflammatory and infectious diseases can also accumulate in this tracer [29]. MRI is superior to CT in the characterization of the internal architecture of lymph nodes, since it can reveal the fatty hilum, borders, and presence of necrosis with high-contrast resolution. By combining the morphological, functional, and metabolic features of suspected lymph nodes, PET/MRI fusion reduces the false-positive rate of stand-alone PET [29]. In addition, PET/MRI fusion can be of great value in detecting metastatic lymph nodes when they are not discernible on morphological imaging, including CT and MRI [4, 30]. Indeed, only morphological and size criteria are commonly adopted to distinguish between benign and malignant lymph nodes (i.e., short-axis diameter >10 mm for an oval lymph node and >8 mm for a round lymph node in the pelvis) [4, 31] (Fig. 5). With regard to M-staging, PET/MRI may provide higher diagnostic accuracy than PET/CT in peculiar anatomical sites, including the brain, liver, and bone, where MRI is able to overcome the limitations of ^{18}F-FDG PET [21]. One straightforward indication for PET/MRI fusion is the detection of metastases in the liver. Owing to the relatively high background ^{18}F-FDG uptake of the liver parenchyma on PET/CT, the detection of liver metastases with low ^{18}F-FDG activity is often impaired, especially in the case of lesions <1 cm in size [23, 32, 33]. Iodinated contrast medium in PET/CT (i.e., ceCT/PET)

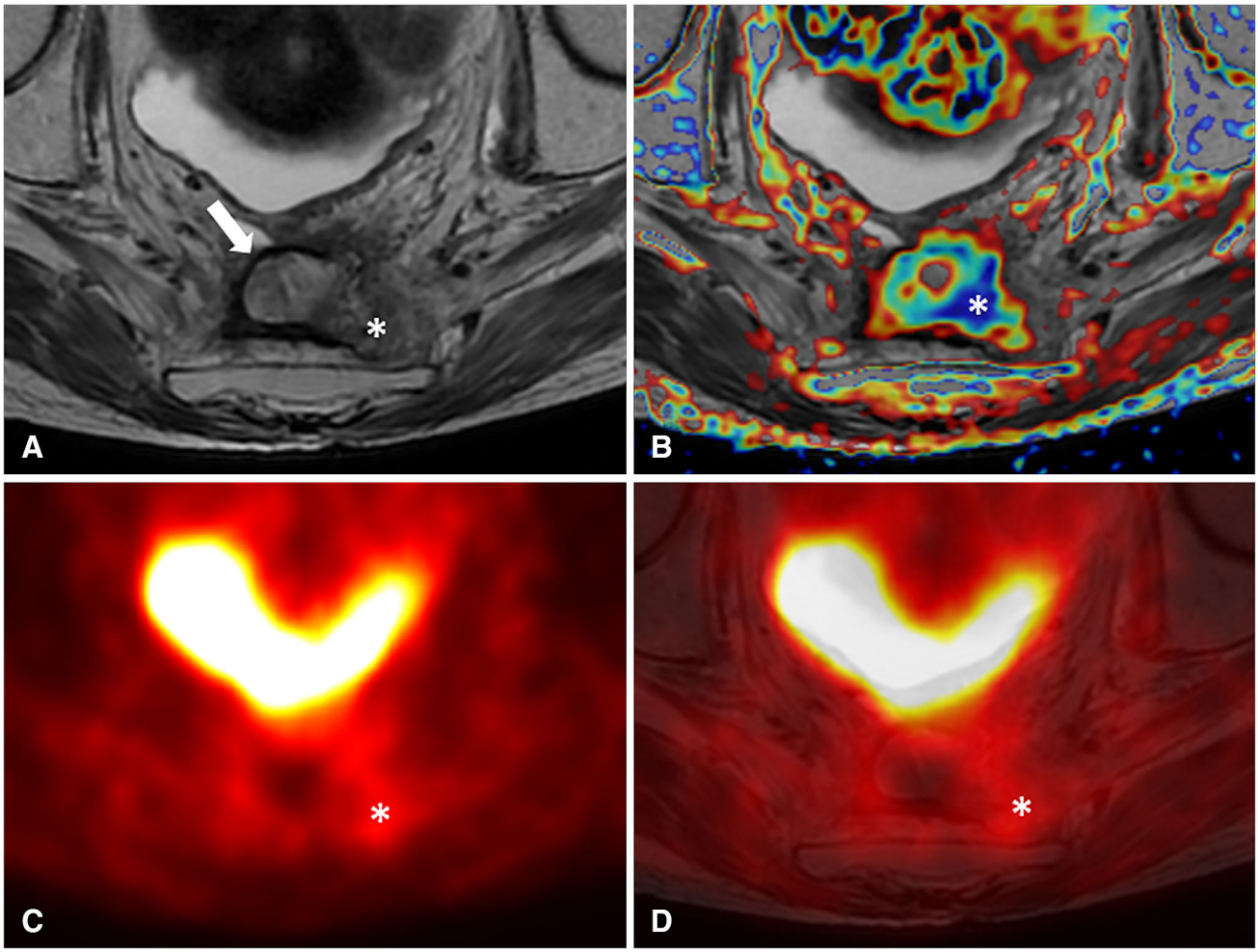

Fig. 4. 67-year-old man who had undergone total mesorectal excision 6 months earlier for an adenocarcinoma of the extraperitoneal rectum. The T2-weighted axial image **A** shows an inhomogeneous area in the presacral space with a semisolid appearance (*arrow*), which was initially interpreted as cancer recurrence. The solid component of the lesion is marked with an asterisk. The ADC map fused and juxtaposed on the T2-weighted image **B** demonstrates that the left lateral portion of the lesion is characterized by restricted water diffusion (*asterisk*). The ^{18}F-FDG PET axial image **C** demonstrates a focal accumulation of the tracer in the presacral space with a SUV_{max} of 2.2 (*asterisk*), which was not considered suggestive of malignancy. The ^{18}F-FDG PET axial scan co-registered with elastic modality and fused with the T2-weighted axial image **D** shows a precise spatial correspondence between the ^{18}F-FDG accumulation and the presacral lesion (*asterisk*). On the basis of the information provided by MMFI, the presacral lesion was interpreted as a post-surgical collection with granulation tissue and was managed conservatively. This finding was dimensionally reduced on a follow-up MRI 1 month later. All images obtained with SmartFusion (Camelot Biomedical Systems, Genoa, Italy).

can improve the detection rate of liver lesions, but, generally, contrast-enhanced MRI with hepatobiliary-specific gadolinium-based contrast agents is considered superior [23, 32, 33]. PET/MRI offers better lesion conspicuity and diagnostic confidence than PET/CT. In a study by Reiner et al. on the detection of liver metastases, PET/MRI displayed significantly higher diagnostic confidence than ceCT/PET [34]; the higher accuracy of PET/MRI was mainly observed in small lesions without increased ^{18}F-FDG uptake. By contrast, the PET component of PET/MRI enables the detection of lesions with absent or low conspicuity on morphological imaging [9] (Fig. 6).

Peculiar applications of multimodal fusion imaging in abdominal and pelvic malignancies

In abdominal applications, the use of specific non-FDG tracers, including radiolabeled somatostatin analogs (^{68}Ga-DOTATOC) and radiolabeled choline derivatives (^{18}F-fluorocholine and ^{11}C-choline), is required for pe-

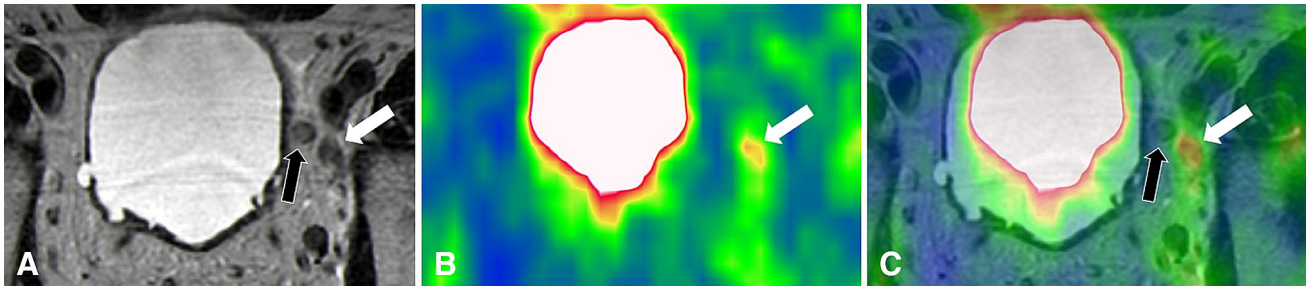

Fig. 5. 76-year-old man who had undergone external beam radiation therapy 11 months earlier for prostate cancer Gleason 7 (3 + 4). Current serum PSA value of 10.1 ng/mL. The T2-weighted axial image **A** shows two small left internal obturator lymph nodes characterized by short-axis diameter <7 mm (*arrow* and *void arrow*). The axial ^{18}F-choline PET image **B** shows an area of intense tracer accumulation in the left aspect of the pelvis. The fused ^{18}F-choline PET/MRI axial image **C** demonstrates that only one lymph node (*arrow*) is characterized by increased metabolic activity. In this patient, who also had a local relapse, the lymph node metastasis was not appreciable on the morphological images, and fusion imaging significantly contributed to identifying another site of recurrence. Images obtained with the co-registration tool of the Virtual Navigator.

culiar tumor types [4, 23]. In the assessment of early liver metastases in neuroendocrine tumors, ^{68}Ga-DOTATOC PET/MRI has shown high diagnostic potential [32].

Fusion imaging between ^{18}F-choline PET and multiparametric MRI has also yielded promising results in prostate cancer patients with biochemical failure after first-line treatment [4, 35–41] (Figs. 7, 8). In a recent paper, Piccardo et al. assessed the diagnostic performance of retrospectively fused ^{18}F-choline PET/MRI in detecting the site of recurrence (i.e., local, lymph nodal or skeletal) in prostate cancer patients who had undergone external beam radiation therapy [4]. On lesion-based analysis, accuracy, sensitivity, and negative predictive value of ^{18}F-choline PET/MRI were significantly higher than those of both multiparametric MRI and CT [4]. Regarding local and lymph node relapse, a significant inverse correlation between ADC and SUV_{max} was noticed [4, 31]. The ADC value measured on DWI sequences and the SUV of ^{18}F-choline PET are imaging parameters that provide quantitative functional and metabolic data that can be effectively combined with the morphological information provided by T2-weighted MRI sequences. The development of size-independent quantitative parameters to assess the metastatic involvement of lymph nodes has great value in patients with prostate cancer, in whom up to 80% of lymph node metastases can be located in normal sized (<8 mm) lymph nodes [31]. However, a major limitation in the clinical application of DWI is the lack of a reliable ADC cut-off value for distinguishing between benign and malignant lymph nodes [4, 31]. The value of retrospectively fused ^{18}F-FDG PET/MRI has also been explored in the field of gynecological malignancies. MRI is routinely performed for accurate T-staging in the preoperative work-up of patients with uterine cervical cancer [29, 30]. In a recent study, Kitajima et al. compared the diagnostic accuracy of retrospectively fused PET/MRI with that of both the separate and side-by-side interpretation of MRI, ^{18}F-FDG PET/CT, ^{18}F-FDG PET/ceCT, and pelvic contrast-enhanced MRI [30]. Fused PET/MRI, side-by-side reading and stand-alone MRI yielded the same diagnostic accuracy of 83.3%, which was superior to that of ^{18}F-FDG PET/ceCT (i.e., 53.3%) [30]. In cervical cancer, ^{18}F-FDG PET/CT is routinely employed for N-staging; this is because it can often detect tiny metastatic lymph nodes from 5 to 9 mm in size, which may not be diagnosed by morphological imaging [29]. In the detection of lymph node metastases, Kim et al. reported sensitivity and specificity values of 44.1% and 93.9% for PET/CT and 54.2% and 92.7% for retrospectively fused PET/MRI; in addition, fused PET/MRI allowed six more metastatic lymph node groups to be detected [29]. Retrospectively fused PET/MRI can also be effectively employed for detecting intra-pelvic recurrence of gynecological tumors, including local relapse, lymph node and bone metastases, and peritoneal dissemination (Fig. 9). A recent comparative study on the diagnostic performance of unenhanced PET/CT, PET/ceCT, contrast-enhanced MRI, and retrospective PET/MRI image fusion demonstrated that the sensitivity of fused PET/MRI in diagnosing local recurrence was significantly better than that of unenhanced PET/CT ($p = 0.041$) [42].

Percutaneous biopsy and ablation therapies under multimodal fusion imaging guidance

The role of imaging guidance in percutaneous minimally invasive interventional procedures is to ensure the precise, effective, and safe placement of medical instruments and devices (i.e., biopsy needles, probes, and catheters) in

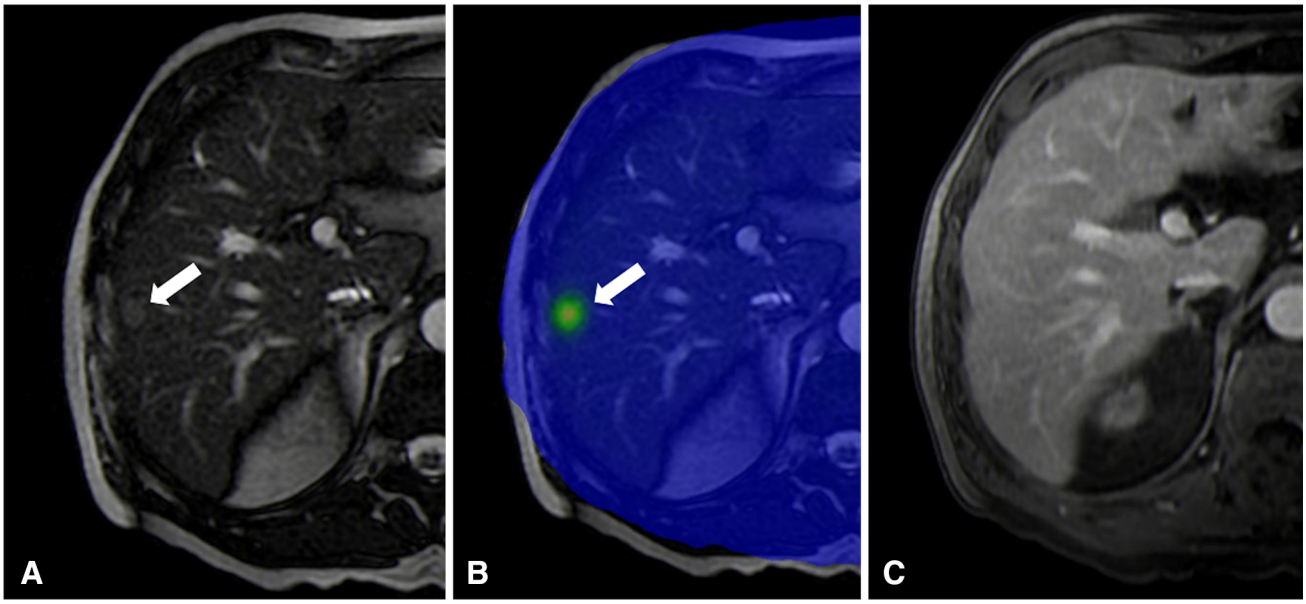

Fig. 6. 56-year-old man who was recently diagnosed with an adenocarcinoma of the sigmoid colon. The FIESTA (fast imaging employing steady-state acquisition) MR image in the axial plane **A** demonstrates a small round slightly hyperintense lesion in the V segment of the liver characterized by very low conspicuity (*arrow*). The bimodal fused ^{18}F-FDG PET/MRI image **B** demonstrates a focal tracer accumulation that corresponds to the subtle MRI finding (*arrow*), which was completely undetectable on the other MRI sequences, including fast spin echo T2-weighted and gadolinium-enhanced LAVA MRI sequences (**C**). Images obtained with the co-registration tool of the Virtual Navigator.

the target lesion [43]. Therefore, imaging guidance is commonly employed for purposes of pre-procedural planning and intra-procedural targeting and monitoring, and there is growing interest in guidance techniques that are able to combine the advantages of different imaging modalities [5, 7].

Advantages and limitations of conventional techniques for image-guided percutaneous biopsy

In routine clinical practice, unenhanced CT and ultrasound are commonly used to guide percutaneous interventional procedures [9]. CT is not a "real-time" guidance modality and provides bi-dimensional axial slices perpendicular to the z-axis. When oblique planes are needed for percutaneous device insertion, gantry angulation can often create adequate windows for safe access to the targeted structure, but only steep angles with respect to the z-axis are permitted in the "off-axis" approach [7]. CT fluoroscopy provides cross-sectional CT images that are reconstructed at reduced spatial resolution and updated continually at a rate of several frames per second. However, this ultrafast technique of acquisition potentially exposes both patients and operators to considerable radiation [44]. Ultrasound is often considered the ideal tool in most solid organs of the abdomen as it enables real-time monitoring of the instrument track to the target lesion (i.e., real-time temporal resolution), is readily available, mobile, and avoids ionizing radiation [5, 7–9]. However, ultrasound cannot always be used to perform image-guided interventions on abdominal lesions, often because of the lack of an adequate access window, or when the target is small, deep, and obscured by superimposed structures that completely reflect the ultrasound beam (i.e., bones or bowel loops) [9]. In addition, the use of this imaging modality is not always feasible owing to limitations in the clear depiction of either the target lesion (i.e., absent or poor conspicuity on B-mode ultrasound images) or the surrounding critical anatomical structures to be avoided (i.e., lack of a comprehensive panoramic view) [9]. Therefore, in such conditions, the operator's ability and experience play a prominent role, and operators may overcome the intrinsic limitations of ultrasound by means of a "mental registration" of the topographical and anatomical information provided by other offline preoperative modalities, such as ceCT, MRI, or PET/CT [9, 45].

Clinical value of real-time multimodal fusion imaging in ultrasound-guided interventional procedures

In selected cases, MMFI platforms can be used to combine the anatomical information from cross-sectional imaging modalities in ultrasound-guided interventional procedures in order to achieve and adequate target/tissue contrast with clear demarcation between the targeted

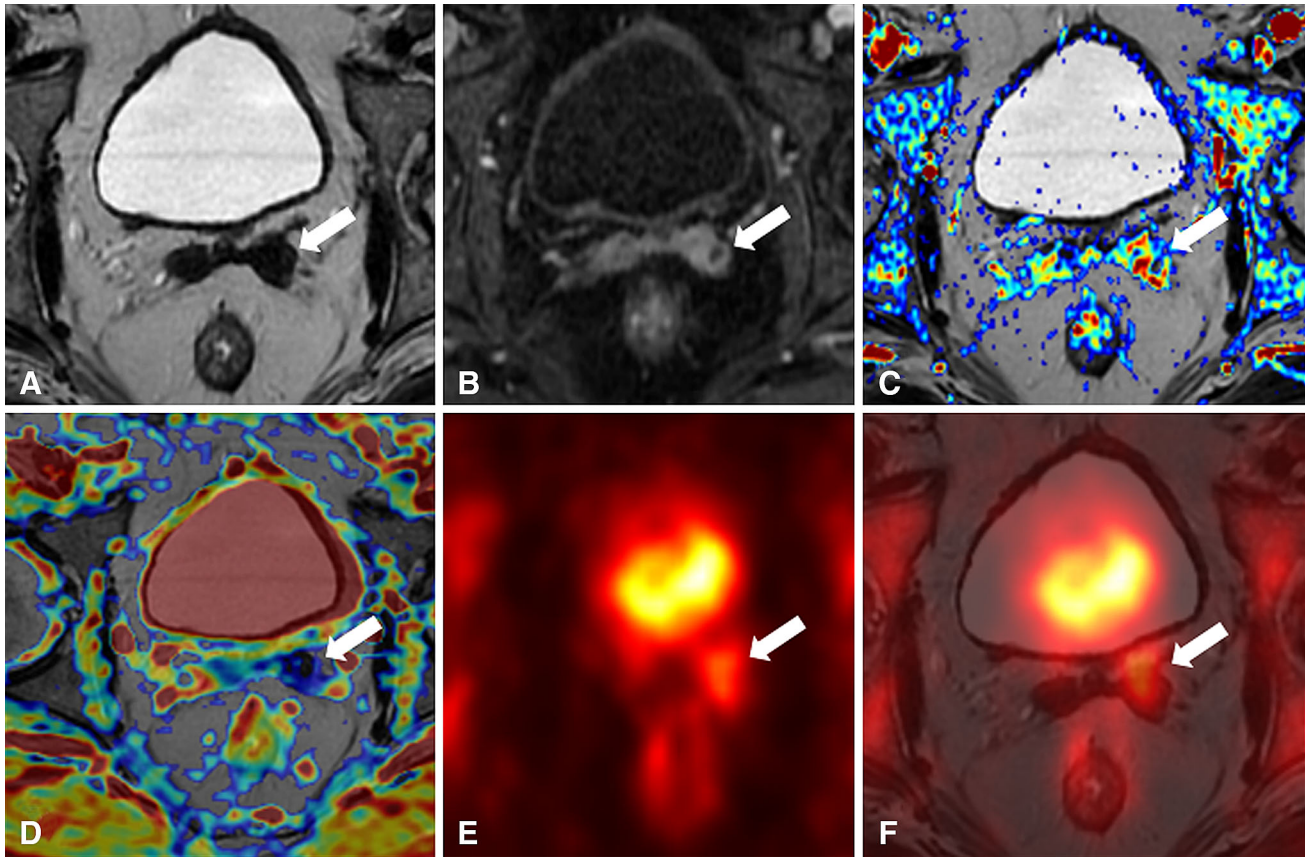

Fig. 7. 75-year-old man treated with radical prostatectomy 7 years earlier for prostate cancer Gleason 7 (3 + 4). Current serum PSA value of 3.5 ng/mL. The T2-weighted axial image **A** shows hypointense nodular thickening of the remnant of the left seminal vesicle (*arrow*), which is hypervascular on both the gadolinium-enhanced LAVA sequence (**B**) and the wash-in perfusion map **C** juxtaposed on the T2-weighted image. The ADC map **D** demonstrates a focal restriction of water diffusion in the remnant of the left seminal vesicle (*arrow*). The axial ^{18}F-choline PET scan **E** shows a focal accumulation of the tracer adjacent to the left posterolateral wall of the urinary bladder (*arrow*). The fused ^{18}F-choline PET/MRI image **F** confirms the spatial correspondence between the focal tracer uptake and the remnant of the left seminal vesicle (*arrow*). Images obtained with the QuantaProstate (Camelot Biomedical Systems, Genoa, Italy).

structure and the surrounding anatomy [3, 5, 7]. Using an MMFI platform (Virtual Navigation System, Esaote Biomedica S.p.A., Genoa, Italy), Mauri et al. performed ablation procedures in 295 hepatic tumors detectable on ceCT or MRI, but completely undetectable by unenhanced B-mode ultrasound and either totally undetectable or poorly conspicuous on contrast-enhanced ultrasound [9]. The rate of successful ablation in these technically challenging targets was very high (90.2%) [9]. ^{18}F-FDG PET/CT is an increasingly important diagnostic tool in oncology; on the basis of PET findings, oncologists are requesting an ever increasing number of interventional procedures, including biopsies and tumor ablations [46]. Recent studies have proposed the use of PET-CT scanners equipped with CT fluoroscopic imaging to assist biopsy procedures in PET-positive lesions [47–49], but these integrated systems are not widely available. Therefore, some authors have proposed the use of MMFI guidance to assist biopsy and ablation procedures in PET-positive targets with low conspicuity on B-mode ultrasound [8, 50–53]. Fusion imaging involving ^{18}F-FDG PET, ceCT, and ultrasound can be effectively used to sample the most metabolically active portion of tumor masses that show uneven tracer accumulation, or to target the most metabolically active lesion among multiple ^{18}F-FDG-avid lesions (e.g., a cluster of lymphadenopathies displaying uneven tracer uptake) [8] (Figs. 10, 11). In the field of prostate cancer, MMFI between multiparametric MRI and transrectal ultrasound (TRUS) has also been used to guide targeted biopsy procedures of suspect lesions detected on multiparametric MRI. According to a recent meta-analysis, multiparametric MRI is characterized by a pooled specificity of 0.88 (95% CI 0.82–0.92) and sensitivity of 0.74 (95% CI 0.66–0.81) for prostate cancer detection, with negative predictive values ranging from 0.65 to 0.94 [54]. Currently, TRUS-guided biopsy is the reference standard for prostate cancer detection, but the detection

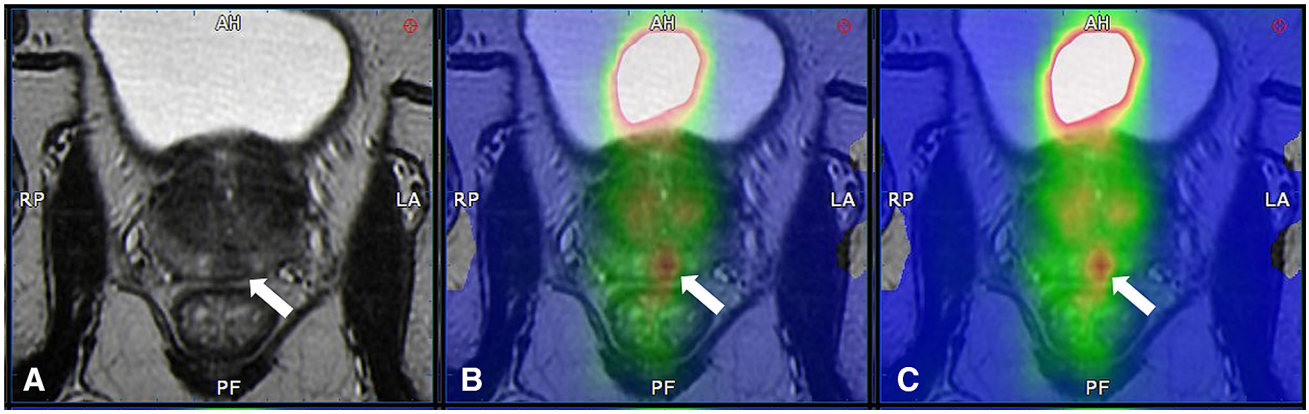

Fig. 8. 72-year-old man with biopsy-proven local recurrence of prostate cancer after external beam radiation therapy. The T2-weighted axial image **A** demonstrates a focal hypointense nodular lesion in the peripheral portion of the gland, close to the mid-line (*arrow*). The bimodal fused ^{18}F-choline PET/MRI images (**B** and **C**) demonstrate, with different degrees of transparency, the precise spatial correspondence between the nodular lesion and a focal accumulation of the ^{18}F-choline tracer (arrows). Images obtained with the co-registration tool of the Virtual Navigator.

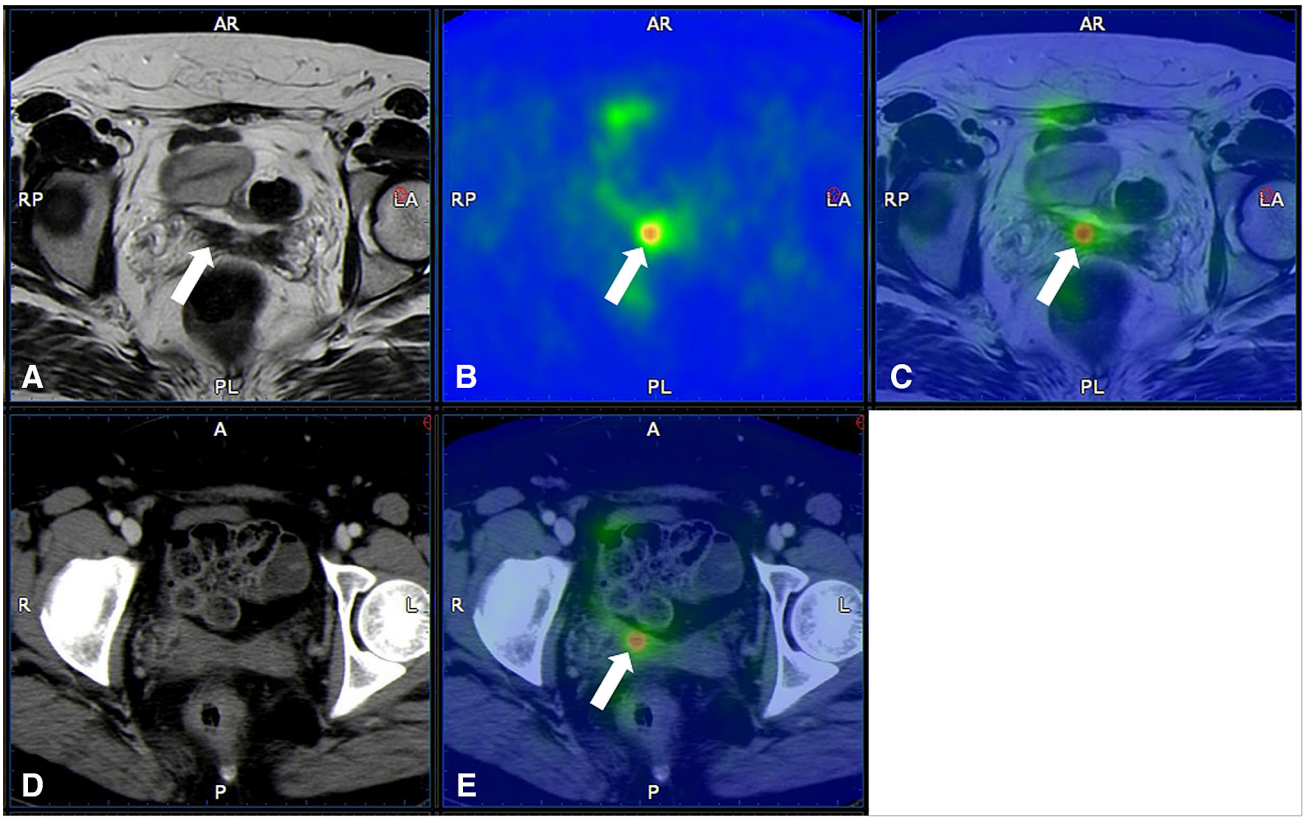

Fig. 9. 42-year-old woman who had undergone hystero-adnexectomy due to an ovarian carcinosarcoma 6 months earlier. The T2-weighted axial MR image **A** shows the upper extremity of the vagina as a low intensity median structure with an irregular appearance (*arrow*). The ^{18}F-FDG PET axial scan **B** shows a focal tracer accumulation in the mid-line of the pelvis (*arrow*) that was considered highly suspect for local recurrence. The bimodal fused ^{18}F-FDG PET/MRI axial image **C** well demonstrates that the focal tracer uptake is located in the right aspect of the upper portion of the vagina (*arrow*). The contrast-enhanced CT **D** of the pelvis does not show any sign of disease recurrence. Bimodal fused ^{18}F-FDG PET/CT axial image (**E**). Images obtained with the co-registration tool of the Virtual Navigator.

rate of random TRUS-guided biopsies does not exceed 44% [55]. EM tracking and multiparametric MRI/TRUS co-registration enable us to combine the real-time intra-procedural monitoring of TRUS with the potential for detection and tissue characterization of multiparametric MRI. On the basis of the most recent literature, the de-

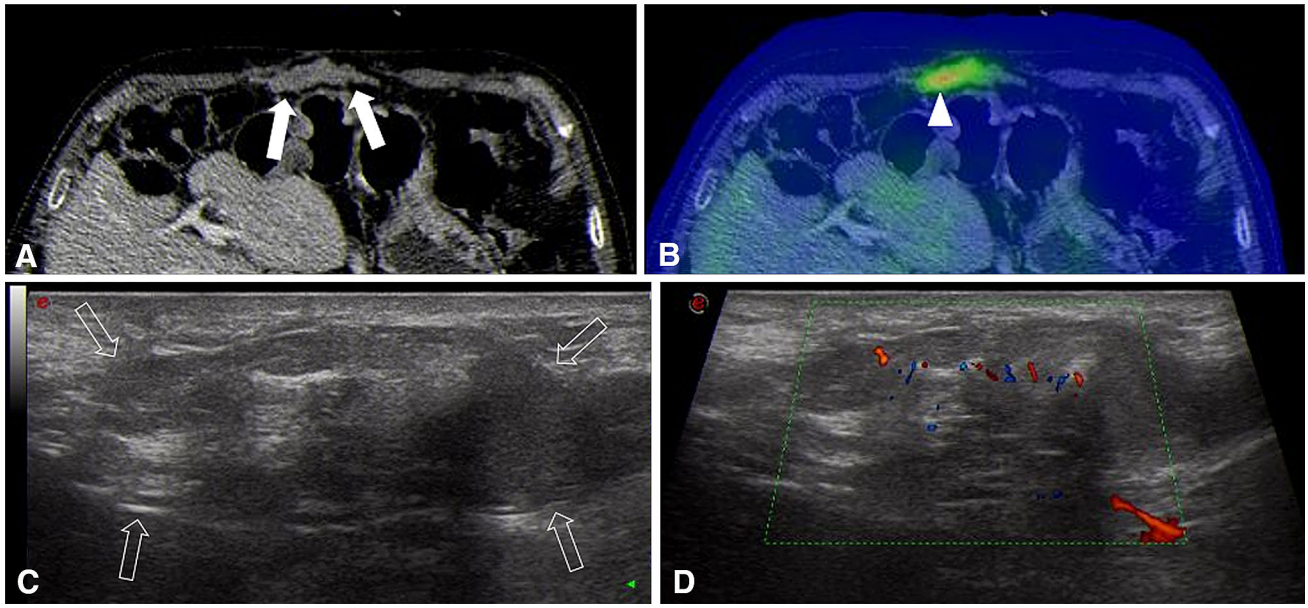

Fig. 10. 80-year-old man who had undergone surgery for an adenocarcinoma of the left colon with liver metastasectomy 5 years earlier. The patient was subsequently treated for a median incisional hernia. On follow-up contrast-enhanced CT (**A**), a thick omental plaque was detected at the site of the mesh repair of the incisional hernia (*arrows*). The ^{18}F-FDG PET/CT fused image **B** demonstrates uneven tracer accumulation that is more evident in the right lateral aspect of the plaque (*arrowhead*) with a SUV_{max} of 6.6. In the transverse ultrasound scan **C**, the omental plaque has the same echogenicity as the surrounding soft tissues and is characterized by some hypervascular signals on color-Doppler (**D**). Images obtained with the Virtual Navigator.

tection rate of prostate biopsy under multiparametric MRI/TRUS MMFI guidance seems to be considerably higher than that of the standard sextant biopsy technique (i.e., up to 80% for clinically significant cancers) [55–57].

Costs, logistics, and limitations

As discussed above, the simultaneous acquisition of MRI and PET images has some intrinsic advantages over the retrospective co-registration of previously acquired image datasets. However, novel integrated PET/MRI systems cost between $5 million and $7 million U.S. (€4.6 million and €6.4 million) [1, 17, 18]. Part of the cost burden is related to the clinical and technical requirements of the installation site. These requirements may include advanced MR applications with dedicated coils for clinical and research purposes and/or high-end PET components, such as new time-of-flight photodetectors, which offer great detection efficiency and excellent spatial, energy, and timing resolution [17, 35, 36]. By comparison, a new-generation PET/CT scanner with 128 detectors costs between $1.5 and $2 million U.S. (€1.4 and €1.8 million) [1, 18]. PET/MRI is yielding promising results in the clinical workflow related to oncological patients. In this regard, PET/MRI may be considered a one-stop-shop modality for the staging and restaging of different types of cancers, while avoiding the risk of cumulative ionizing radiation. The main logistic limitations to the wide clinical implementation of this novel hybrid technology are costs and space availability [1, 17, 36]. Indeed, PET-MRI systems require a slightly larger physical environment than commercially available 3T MRI systems. Software platforms for the retrospective co-registration of previously acquired image sets are a low cost alternative to PET/MRI systems. Commercially available software platforms for retrospective MMFI cost between $10,800 U.S. (€10,000) and $54,000 U.S. (€50,000). They need to be connected to a single or multicenter PACS (Picture archiving and communication system) in order to guarantee rapid download of the input data required for the co-registration process [4, 41]. The main limitation of this MMFI technique is that image sets have been acquired at different times, and thus only partially compensate for different physiological conditions [4, 15]. Software platforms for the real-time co-registration of ultrasound images with previously acquired cross-sectional imaging modalities are implemented in various high-end multipurpose ultrasound systems [8]. One of the least expensive systems equipped with the virtual navigator technology costs approximately $100,000 U.S. (€95,000) [9]. It may be used for all the conventional clinical applications of ultrasonography as well as for guiding ablation and biopsy procedures on technically challenging targets, with particular regard to PET-positive lesions with absent or low conspicuity on morphological imaging [8]. Without this

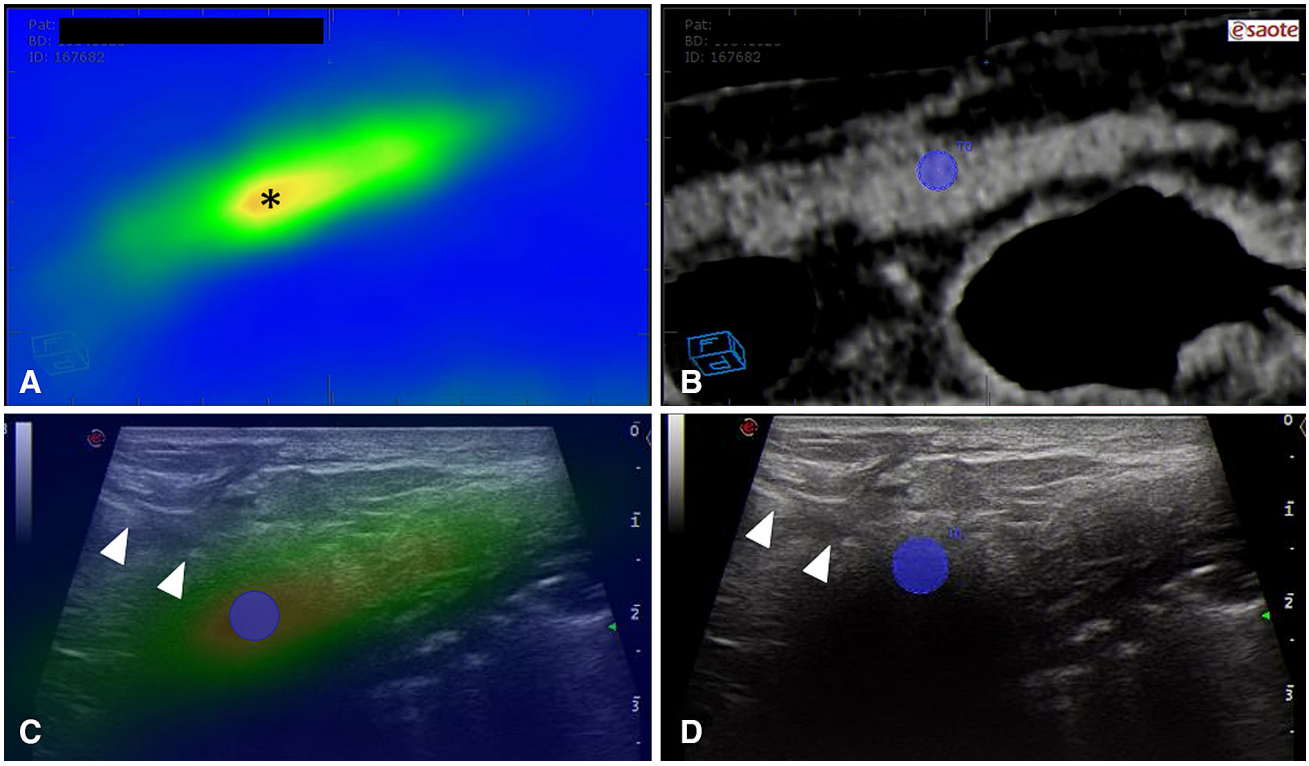

Fig. 11. Same patient as Fig. 10. Biopsy procedure of the PET-positive omental plaque under real-time ^{18}F-FDG PET-CT/ultrasound fusion imaging guidance. The ^{18}F-FDG PET scan **A** demonstrates the most metabolically active portion of the lesion (*asterisk*). Once trimodal ^{18}F-FDG PET-CT/ultrasound image fusion had been finalized—using internal anatomical landmarks for the co-registration process—a round *blue marker* was placed on the contrast-enhanced CT (**B**) at the biopsy site. The marker is simultaneously displayed on both the bimodal ^{18}F-FDG PET/ultrasound fused image (**C**) and the B-mode ultrasound image (**D**). The display of the Virtual Navigator allowed us to monitor in real-time the track of a semiautomatic biopsy needle (*arrowheads* in **C** and **D**) toward the targeted area of the omental plaque. The histological analysis of the biopsy specimens did not reveal the presence of cancer cells but only fibroinflammatory and granulation tissue. Images obtained with the Virtual Navigator platform implemented on the MyLab Twice ultrasound system (Esaote Biomedica, Genoa, Italy).

novel technology, many of these patients would have been referred to more invasive treatments (such as surgery); alternatively, more expensive and potentially harmful imaging modalities (i.e., CT, MRI or fluoroscopy) would have had to be used for guiding ablative and biopsy procedures.

However, the co-registration process of real-time ultrasound scans with previous PET/CT and ceCT images is not straightforward, requires well-trained operators and may be time-consuming, particularly when different image sets have been acquired in different phases of the respiratory cycle [3, 8, 9].

Conclusions

Medicine is evolving toward personalized care and this development entails the integration, amalgamation, and synchronized analysis of data from multiple sources. A common problem experienced by radiologists working in clinical facilities is the time wasted on moving between different applications and workstations to perform routine image analysis of multimodality diagnostic datasets. PET/MRI scanners and MMFI platforms are able to improve the diagnostic workflow in oncologic patients and provide exquisite images that aid physicians in the molecular profiling and characterization of tissues. Advanced navigation platforms involving real-time ultrasound are promising tools for guiding personalized and tailored mini-invasive interventional procedures on technically challenging targets.

References

1. Beyer T, Freudenberg LS, Townsend DW, Czernin J (2011) The future of hybrid imaging-part 1: hybrid imaging technologies and SPECT/CT. Insights Imaging 2:161–169
2. Indrajit I, Verma B (2009) Monitor displays in radiology: Part 1. Indian J Radiol Imaging 19:24–28
3. Ewertsen C, Săftoiu A, Gruionu LG, Karstrup S, Nielsen MB (2013) Real-time image fusion involving diagnostic ultrasound. AJR Am J Roentgenol 200:249–255
4. Piccardo A, Paparo F, Picazzo R, et al. (2014) Value of fused 18F-Choline-PET/MRI to evaluate prostate cancer relapse in patients showing biochemical recurrence after EBRT: preliminary results. Biomed Res Int 2014:103718

5. Abi-Jaoudeh N, Kruecker J, Kadoury S, et al. (2012) Multimodality image fusion-guided procedures: technique, accuracy, and applications. Cardiovasc Intervent Radiol 35:986–998
6. Slomka PJ, Baum RP (2009) Multimodality image registration with software: state-of-the-art. Eur J Nucl Med Mol Imaging 36(1):44–55
7. Appelbaum L, Mahgerefteh SY, Sosna J, Goldberg SN (2013) Image-guided fusion and navigation: applications in tumor ablation. Tech Vasc Interv Radiol 16:287–295
8. Mauri G, Cova L, De Beni S, et al. (2015) Real-time US-CT/MRI image fusion for guidance of thermal ablation of liver tumors undetectable with US: results in 295 cases. Cardiovasc Intervent Radiol 38:143–151
9. Paparo F, Piccazzo R, Cevasco L, et al. (2014) Advantages of percutaneous abdominal biopsy under PET-CT/ultrasound fusion imaging guidance: a pictorial essay. Abdom Imaging 39:1102–1113
10. James PA, Dasarathy BV (2014) Medical image fusion: a survey of the state of the art. Inf Fusion 19:4–19
11. Woods RP, Grafton ST, Holmes CJ, Cherry SR, Mazziotta JC (1998) Automated image registration: I. General methods and intrasubject, intramodality validation. J Comput Assist Tomogrv 22:139–152
12. Giesel FL, Mehndiratta A, Locklin J, et al. (2009) Image fusion using CT, MRI and PET for treatment planning, navigation and follow up in percutaneous RFA. Exp Oncol 31:106–114
13. Zitova Barbara, Flusser Jan (2003) Image registration methods: a survey. Image Vis Comput 21:977–1000
14. Wood BJ, Kruecker J, Abi-Jaoudeh N, et al. (2010) Navigation systems for ablation. J Vasc Interv Radiol 21(8):257–263
15. Maccioni F, Patak MA, Signore A, Laghi A (2012) New frontiers of MRI in Crohn's disease: motility imaging, diffusion-weighted imaging, perfusion MRI, MR spectroscopy, molecular imaging, and hybrid imaging (PET/MRI). Abdom Imaging 37:974–982
16. Appelbaum L, Solbiati L, Sosna J, et al. (2013) Evaluation of an electromagnetic image-fusion navigation system for biopsy of small lesions: assessment of accuracy in an in vivo swine model. Acad Radiol 20:209–217
17. Beyer T, Townsend DW, Czernin J, Freudenberg LS (2011) The future of hybrid imaging-part 2: PET/CT. Insights Imaging 2:225–234
18. Beyer T, Freudenberg LS, Czernin J, Townsend DW (2011) The future of hybrid imaging-part 3: PET/MR, small-animal imaging and beyond. Insights Imaging 2:235–246
19. von Schulthess GK, Kuhn FP, Kaufmann P, Veit-Haibach P (2013) Clinical positron emission tomography/magnetic resonance imaging applications. Semin Nucl Med 43:3–10
20. Hofmann M, Steinke F, Scheel V, et al. (2008) MRI-based attenuation correction for PET/MRI: a novel approach combining pattern recognition and atlas registration. J Nucl Med 49:1875–1883
21. Jadvar H, Colletti PM (2014) Competitive advantage of PET/MRI. Eur J Radiol 83:84–94
22. Teixera SR, Kohan AA, Paspulati RM, Rong R, Herrmann KA (2014) Potential role of positron emission tomography/magnetic resonance imaging in gastrointestinal and abdominal malignancies: preliminary experience. Semin Roentgenol 49:321–333
23. Nensa F, Beiderwellen K, Heusch P, Wetter A (2014) Clinical applications of PET/MRI: current status and future perspectives. Diagn Interv Radiol 20:438–447
24. Crocetti L, Lencioni R, Debeni S, et al. (2008) Targeting liver lesions for radiofrequency ablation: an experimental feasibility study using a CT-US fusion imaging system. Invest Radiol 43:33–39
25. Di Mauro E, Solbiati M, De Beni S, et al. (2013) Virtual navigator real-time ultrasound fusion imaging with positron emission tomography for liver interventions. Conf Proc IEEE Eng Med Biol Soc 2013:1406–1409
26. Wood BJ, Zhang H, Durrani A, et al. (2005) Navigation with electromagnetic tracking for interventional radiology procedures: a feasibility study. J Vasc Interv Radiol 6:493–505
27. Racadio JM, Babic D, Homan R, et al. (2007) Live 3D guidance in the interventional radiology suite. AJR Am J Roentgenol 189:357–364
28. Tam A, Mohamed A, Pfister M, Rohm E, Wallace MJ (2009) C-arm cone beam computed tomographic needle path overlay for fluoroscopic-guided placement of translumbar central venous catheters. Cardiovasc Intervent Radiol 32:820–824
29. Kim SK, Choi HJ, Park SY, et al. (2009) Additional value of MR/PET fusion compared with PET/CT in the detection of lymph node metastases in cervical cancer patients. Eur J Cancer 45:2103–2109
30. Kitajima K, Suenaga Y, Ueno Y, et al. (2014) Fusion of PET and MRI for staging of uterine cervical cancer: comparison with contrast-enhanced (18)F-FDG PET/CT and pelvic MRI. Clin Imaging 38:464–469
31. Beer AJ, Eiber M, Souvatzoglou M, et al. (2011) Restricted water diffusibility as measured by diffusion-weighted MR imaging and choline uptake in (11)C-choline PET/CT are correlated in pelvic lymph nodes in patients with prostate cancer. Mol Imaging Biol 13:352–361
32. Schreiter NF, Nogami M, Steffen I, et al. (2012) Evaluation of the potential of PET-MRI fusion for detection of liver metastases in patients with neuroendocrine tumours. Eur Radiol 22:458–467
33. Beiderwellen K, Gomez B, Buchbender C, et al. (2013) Depiction and characterization of liver lesions in whole body [18F]-FDG PET/MRI. Eur J Radiol 82:669–675
34. Reiner CS, Stolzmann P, Husmann L, et al. (2014) Protocol requirements and diagnostic value of PET/MR imaging for liver metastasis detection. Eur J Nucl Med Mol Imaging 41:649–658
35. Wetter A, Nensa F, Schenck M, et al. (2014) Combined PET imaging and diffusion-weighted imaging of intermediate and high-risk primary prostate carcinomas with simultaneous [18F] choline PET/MRI. PLoS One 9:101571
36. Hartenbach M, Hartenbach S, Bechtloff W, et al. (2014) Combined PET/MRI improves diagnostic accuracy in patients with prostate cancer: a prospective diagnostic trial. Clin Cancer Res 20:3244–3253
37. Wetter A, Lipponer C, Nensa F, et al. (2014) Quantitative evaluation of bone metastases from prostate cancer with simultaneous [18F] choline PET/MRI: combined SUV and ADC analysis. Ann Nucl Med 28:405–410
38. Wetter A, Lipponer C, Nensa F, et al. (2014) Evaluation of the PET component of simultaneous [(18)F]choline PET/MRI in prostate cancer: comparison with [(18)F]choline PET/CT. Eur J Nucl Med Mol Imaging 41:79–88
39. Wetter A, Lipponer C, Nensa F, et al. (2013) Simultaneous 18F choline positron emission tomography/magnetic resonance imaging of the prostate: initial results. Invest Radiol 48:256–262
40. Arce-Calisaya P, Souvatzoglou M, Eiber M, et al. (2013) Sensitivity of PET/MRI to detect recurrence of prostate cancer. Eur J Nucl Med Mol Imaging 40:799
41. Paparo F, Piccardo A, Bacigalupo L, et al. (2015) Value of bimodal (18)F-choline-PET/MRI and trimodal (18)F-choline-PET/MRI/TRUS for the assessment of prostate cancer recurrence after radiation therapy and radical prostatectomy. Abdom Imaging. doi: 10.1007/s00261-014-0345-0
42. Kitajima K, Suenaga Y, Ueno Y, et al. (2014) Value of fusion of PET and MRI in the detection of intra-pelvic recurrence of gynecological tumor: comparison with 18F-FDG contrast-enhanced PET/CT and pelvic MRI. Ann Nucl Med. 28:25–32
43. Helmberger T, Martí-Bonmatí L, Pereira P, et al. (2013) Radiologists' leading position in image-guided therapy. Insights Imaging 4:1–7
44. Carlson SK, Bender CE, Classic KL, et al. (2001) Benefits and safety of CT fluoroscopy in interventional radiologic procedures. Radiology 219:515–520
45. Liu FY, Yu XL, Liang P, et al. (2012) Microwave ablation assisted by a real-time virtual navigation system for hepatocellular carcinoma undetectable by conventional ultrasonography. Eur J Radiol 81:1455–1459
46. Kobayashi K, Bhargava P, Raja S, et al. (2012) Image-guided biopsy: what the interventional radiologist needs to know about PET/CT. Radiographics 32:1483–1501
47. Tatli S, Gerbaudo VH, Mamede M, et al. (2010) Abdominal masses sampled at PET/CT-guided percutaneous biopsy: initial experience with registration of prior PET/CT images. Radiology 256:305–311
48. Tatli S, Gerbaudo VH, Feeley CM, et al. (2011) PET/CT-guided percutaneous biopsy of abdominal masses: initial experience. J Vasc Interv Radiol 22:507–514
49. Gupta S, Madoff DC (2007) Image-guided percutaneous needle biopsy in cancer diagnosis and staging. Tech Vasc Interv Radiol 10:88–101

50. Ewertsen C (2010) Image fusion between ultrasonography and CT, MRI or PET/CT for image guidance and intervention - a theoretical and clinical study. Dan Med Bull 57:4172
51. Ewertsen C, Henriksen BM, Torp-Pedersen S, Bachmann Nielsen M (2011) Characterization by biopsy or CEUS of liver lesions guided by image fusion between ultrasonography and CT, PET/CT or MRI. Ultraschall Med 32:191–197
52. Venkatesan AM, Kadoury S, Abi-Jaoudeh N, et al. (2011) Real-time FDG PET guidance during biopsies and radiofrequency ablation using multimodality fusion with electromagnetic navigation. Radiology 260:848–856
53. Krücker J, Xu S, Venkatesan A, et al. (2011) Clinical utility of real-time fusion guidance for biopsy and ablation. J Vasc Interv Radiol 22:515–524
54. de Rooij M, Hamoen EH, Fütterer JJ, Barentsz JO, Rovers MM (2014) Accuracy of multiparametric MRI for prostate cancer detection: a meta-analysis. AJR Am J Roentgenol 202:343–351
55. Logan JK, Rais-Bahrami S, Turkbey B, et al. (2014) Current status of magnetic resonance imaging (MRI) and ultrasonography fusion software platforms for guidance of prostate biopsies. BJU Int 114:641–652
56. Marks L, Young S, Natarajan S (2013) MRI-ultrasound fusion for guidance of targeted prostate biopsy. Curr Opin Urol 23: 43–50
57. Siddiqui MM, Rais-Bahrami S, Turkbey B, et al. (2015) Comparison of MR/ultrasound fusion-guided biopsy with ultrasound-guided biopsy for the diagnosis of prostate cancer. JAMA 313:390–397